A Spring-Loaded Chip Interface for Flexible Stripline Cryogenic Readout

L. H. Marting, N. de Keijzer, N. Drobotun, J. M. de Voogd, T. de Bondt, R. Huiting, R. Groefsema, and J. J. A. Baselmans

***Abstract*—Scaling astronomical detectors and quantum devices to larger and larger sizes will require more readout lines. A problem with extra readout lines is the complexity and cost of many coaxial cables in parallel. Furthermore, the thermal loading on the coldest stages via thermal conductivity should be kept at a minimum. Delft circuits provides an eight-channel flexible cabling solution based on stripline technology with Ag or NbTi conductors and polyimide dielectric (flexline) as a solution to these problems. However, a compact and light-tight flex-to-chip interface is lacking, and this would be key to unlocking its full scaling and lightweight potential. Here, we present the design and measurements of a flexline to PCB interface for cryogenic detectors. The flexline is connected securely via a spring-loaded pressing tool, ensuring reliable contact even after thermal contraction. To reduce stray radiation, the chip and connector assembly sits in a light-tight setup. The connector spans a width of 20 mm along one edge of the chip, illustrating the compact design. We show that the flexline connector has an insertion loss of –2 dB at 7 GHz using a probe measurement at room temperature. We also demonstrate the connector with a test chip with kinetic inductance detectors in a dilution refrigerator cooled to 40 mK.**

***Index Terms*—Cryogenic electronics, superconducting cables, superconducting filaments and wires, superconducting resonators, superconducting microwave devices.**

I. Introduction

QUANTUM devices, such as large qubit systems [1], [2], [3], [4], [5] or astronomical instruments [6], [7], [8], [9], [10], have been steadily growing in size. These systems have typically used coaxial cables for their readout system, but this is nearing the limit of scalability. The footprint of each cable creates logistical complexity of mounting all these cables, attenuators, DC blocks and other inline components at each stage to properly thermalize them. If one cable has an issue, this might mean removing 30 other cables to address it.

Received 26 September 2025; revised 8 January 2026; accepted 13 January 2026. Date of publication 25 February 2026; date of current version 2 April 2026. This work was supported by Quantum Delta NL. *(Corresponding author: L. H. Marting.)*

L. H. Marting and J. J. A. Baselmans are with the Delft University of Technology, 2628 Delft, The Netherlands, and also with the SRON Space Research Organization Netherlands, 3584 Utrecht, The Netherlands (e-mail: l.h.marting@tudelft.nl).

N. de Keijzer, R. Huiting, and R. Groefsema are with the SRON Space Research Organization Netherlands, 3584 Utrecht, The Netherlands.

N. Drobotun and J. M. de Voogd are with Delft Circuits, 2627 Delft, The Netherlands.

T. de Bondt is with Leiden Cryogenics, 2331 Leiden, The Netherlands.

Color versions of one or more figures in this article are available at https://doi.org/10.1109/TASC.2026.3668003.

Digital Object Identifier 10.1109/TASC.2026.3668003

Furthermore, such large cable trees would put excessive thermal loading at the cold stages, especially at temperatures T >10 K where superconducting cables cannot be used, which would allow low thermal conduction without any signal attenuation. With nonsuperconducting cables these are always inversely related through the Wiedemann–Franz law [11]. Large instruments, such as experiments targeting the cosmic microwave background which rely on having large detector counts [6], could benefit from a reduction in thermal loading, which allows more detectors to be used in the same cryogenic hardware.

Moreover, the inner dielectrics of the coaxial cables are typically transparent up to far-infrared (FIR) wavelengths, causing radiation leakage to the coldest stages, which needs extra components to filter out, further increasing complexity. It is clear that an alternative is needed to the conventional coaxial cabling for large-scale cryogenic systems.

Solutions exist in the form of ribbon cables [12], [13] and the Cri/oFlex® cables of Delft-Circuits. The latter is a eight-line flexible ribbon-cable solution based on stripline technology with Ag or NbTi conductors and polyimide dielectric [14], [15]. Both these systems reduce the footprint of the readout hardware significantly. The coaxial ribbons can be connected to a sample holder readily using G3PO connectors, as shown in [13]. For the flexline of Delft Circuits such a solution is not available.

Here we present a design of a Delft Circuits flexline-to-chip interface. The interface is designed to have a light-tight throughput, it ensures robust connection even at cryogenic temperatures and it allows chips to be interchanged easily. We measure the isolated flexline connector at room temperature and we demonstrate the connector at cryogenic temperatures.

II. Design of Flexline–Chip Interface

A standard Delft Circuits Cri/oFlex© flexline is a stripline with 2 μm thick silver or silver-coated NbTi signal traces, which are separated by 1 mm. The ground plane is separated from the signal traces by a polyimide laminate substrate of approximately 120 μm thick. It is fabricated as follows; the signal traces are deposited and patterned on a polyimide substrate. This is sandwiched between two other polyimide substrates with a ground plane on the outer edge, consisting of the same material as the conductors. A thin layer of glue is used to hold this lamination in place. Finally, via holes are fabricated through the full stack where needed. This stratification is protected by a final polyimide layer on both sides and is also attached using a thin glue layer. The flexline fabrication allows the removal of

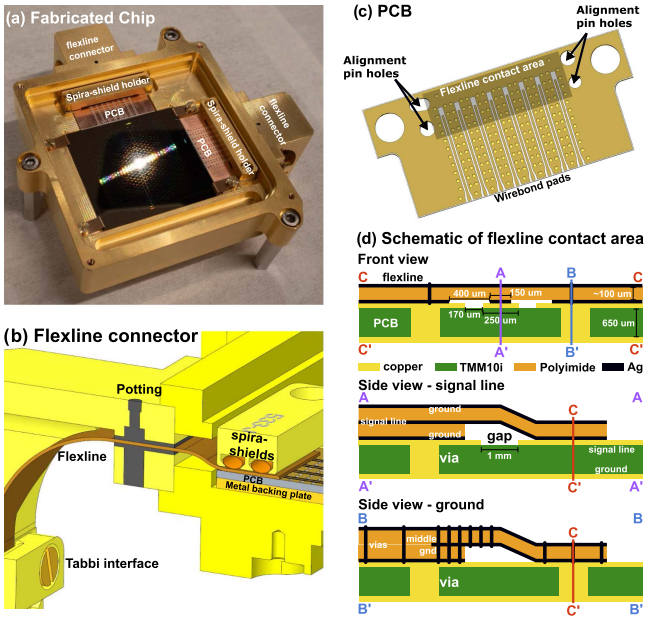

Fig. 1. (a) Fabricated flexline connector and chip holder. (b) Flexline connector cross-section. (c) PCB with alignment holes and traces for flex to PCB transition. (d) Schematic of the flexline contact area. The PCB signal trace is wider by 400 μm, which gives some alignment tolerance to the design.

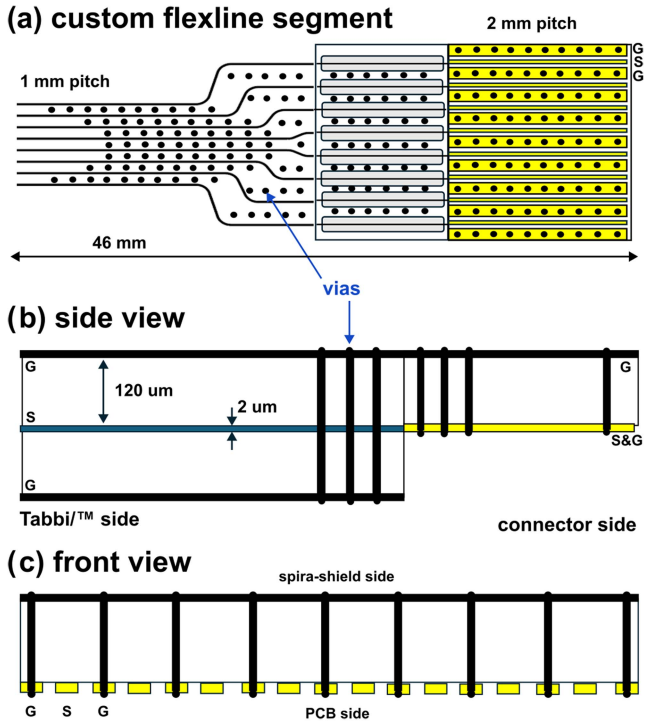

Fig. 2. (a) Schematic drawing of the custom flexline element that is part of the connector as shown in Fig. 1. (b) Side-view of the component. On the left is a standard stripline. In the middle the top and bottom grounds are connected using vias. On the right, at the connector side, the center signal trace with co-planar ground traces is exposed to connect to the PCB. (b) Front view at the connector side, showing how each signal trace is isolated using ground vias.

one side of the ground plane and dielectric substrate at both ends of the wire, exposing the signal traces.

For our flexline connector, there are several constraints that the design must adhere to. First, the design must function under cryogenic temperatures down to 20 mK. The thermal contraction of the polyimide substrate is our main concern, which is significantly larger than for metals, resulting in a much stronger shrink of the flexline than any metallic housing. This poses an issue with reliably contacting the signal traces to other components, since the contraction might shift or dislodge the flexline causing a bad connection. Second, it must still be possible to swap chips without needing to touch the flexline connector. This constraint requires us to use a PCB to connect to the chip, since it is a reliable platform to wirebond to the chips from. We will therefore make the flexline transition connect to the PCB. Finally, the flexline connection to the chip holder must reduce stray light to a minimum.

Given these constraints, we have designed the custom flexline connector, as shown in Fig. 1. The flexline connects to the PCB using a spring-loaded pressing system, which is implemented using Spira-shields [16]. The Spira-shields apply a force to the backside of the flexline at two points: at the ground plane and at the signal lines of the flexline to the PCB. This spring system guarantees that a reliable force is applied to the contact between flexline and PCB, even at cryogenic temperatures where thermal contraction would cause a normal press-fit to become unreliable. Furthermore, it ensures that the flexline is bent down to make the contact with the signal lines on the PCB. We used the low-force variant of the Spira-shield with a diameter of 1.6 mm, which has a force of 1.5 pounds per inch length or 0.263 N mm^{-1}. This force is provided for a recommended indentation of 25% of the Spira-shield diameter, which is equivalent to a spring travel of 400 μm. We have two Spira-shields of 22 mm long each, giving a total force of 11.6 N.

To reduce cross-talk between CPW lines on the PCB, grounding vias in the PCB between the densely placed CPW trace are required. These vias require at least an area of 400 μm in diameter to be fabricable, resulting in a signal trace pitch of 2 mm. Furthermore, a line pitch of 2 mm allows for enough spacing between wirebond pads.

A dedicated custom flexline is designed for the flexline to the PCB interface with a standard 1 mm pitch on the cable connector (Tabbi/$^{\text{TM}}$2Flex) at one side, and a 2 mm pitch at the connection to the circuit board, as shown in Fig. 2. Grounding vias in the flexline keep the top-ground properly grounded through the transition to the PCB. Four alignment pins are used to align the flexline with the PCB using the edges of the flexline, which are manufactured by high-precision machining. the alignment pins sit in the metal backing plate, which is soldered to the PCB. The eight signal lines span 16 mm on the edge of the chip, this compact form allows very dense arrays to be connected easily.

This design was simulated in CST, a commercial EM solver, to calculate and optimize the transmission across the flexline connector. The brown dashed line in Fig. 4 shows the simulated transmission. We get a transmission loss that is less than 1 dB up to 8 GHz. This is decent but not as good as a coaxial line, which has a nearly flat transmission in this range. This loss is dominated by the metal losses of the signal traces, with a small contribution of dielectric losses [we use polyimide ($\tan\delta \approx 1 \times 10^{-2}$),

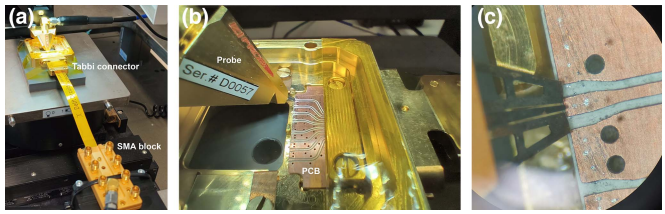

Fig. 3. (a) Probe station measurement setup. The flexline is connected to an extra section of flexline with an SMA block; this section is deembedded in post processing using the IEEE 370 standard. (b) Flexline connector with probe landed on the PCB. NB: this figure shows an older iteration of the PCB with a narrower signal wire pitch and less ground vias. (c) Microscope image of the landed probe.

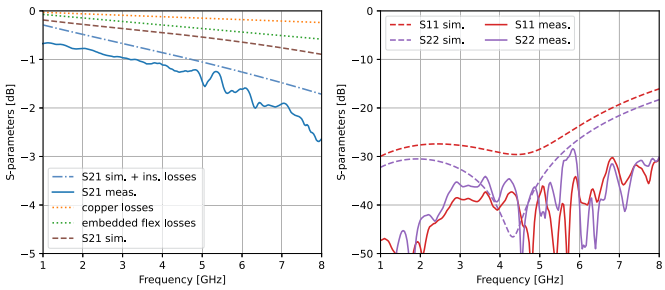

Fig. 4. De-embedded S-parameters of the flexline connector averaged across the seven nominal channels (channel 5 had a defect). Port 1 is the probe tip, port 2 is the Tabbi/$^{\mathrm{TM}}$2Flex connector. The left graph shows the average transmission of the flexline connector from tabbi connector to PCB edge (solid) compared to the simulation (dot-dash). The dotted lines give an indication of the expected losses in the copper and the embedded flexline. The dashed line is the expected transmission of the connector only from simulations. The right graph shows the measured reflections of the structure (solid) compared to the simulations (dashed).

which is more lossy than Teflon/PTFE ($\tan\delta \approx 2 \times 10^{-4}$) and is typically used in coaxial cables]. An NbTi flexline for superconducting lines will not completely solve this problem because the flexline fabrication requires a normal metal coating layer for adhesion to the polyimide to ensure long-term reliability.

Finally, a slit structure with a stycast potting creates a light-tight feed-through for the flexline. The stycast of type 2050FT is laced with copper powder to create a lossy epoxy to block thermal radiation at FIR and terahertz frequencies. In addition, it secures the flexline to the chip-holder.

III. Probe-Station Measurement

We first measure the flexline connector using a probe-station to verify the transmission of our structure. The probe-station measurement setup can be seen in Fig. 3. The probe station measurement gives us a representative measurement of the connector because the probe is landed where normally the chip would be wirebonded.

The measurement is performed from 1 to 8 GHz and is repeated eight times, once for each signal trace. We calibrated the measurement setup in two stages. First, the SMA cables from the VNA are calibrated with standard references. Then, the probe is calibrated with a one-port short-open-load calibration and the reference plane for the probe is moved to the tips of the probe.

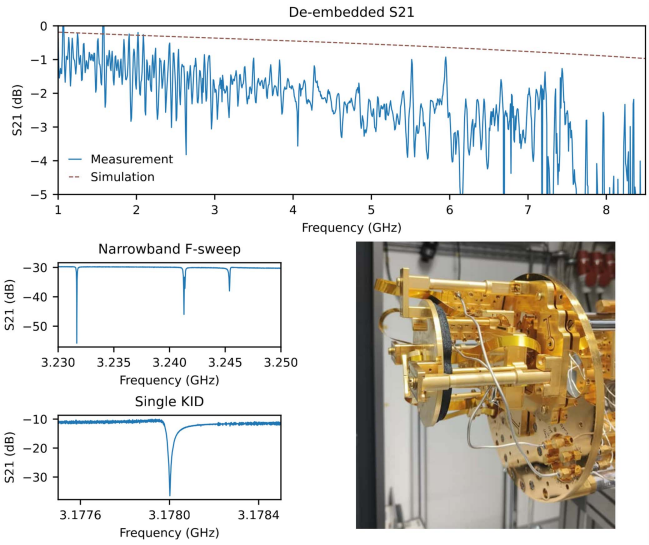

Fig. 5. Results of the cryogenic measurement of the flexline connector. The dashed line labeled *simulation* is equal to the simulated S21 in Fig. 4. The KID sweeps are not de-embedded. The bottom-right image shows the flexline connector mounted in the cryostat.

This is port 1. The other SMA cable connects to the SMA block and this is port 2.

The measurement results of the probe measurement can be seen in Fig. 4. The solid line shows the average transmission of our flexline connector, which we can compare to the dash-dotted line. The dash-dotted line is the predicted transmission given our simulation and with the resistive and dielectric losses at room temperature of the copper PCB and the polyimide. Our measurements are within 1 dB of the predicted transmission, typically being about 0.5 dB lower, with a taper to a larger difference at 8 GHz to 1 dB difference. The reflections are low across the band. We attribute the losses to contact losses between the surface of the flexlines and the copper PCB.

IV. Cryogenic Measurement

We also measured the flexline connector in a cryostat with a dilution unit with the mixing chamber plate at 40 mK to verify that it works in its intended cryogenic environment. The chip and holder are mounted at the 40 mK mixing chamber plate and connected to two SMA blocks via the Tabbi/$^{\mathrm{TM}}$2Flex connectors, also on the mixing chamber plate. This is connected to the rest of the system via an existing coaxial readout chain. The chip has an array of kinetic inductance detectors (KIDs) on it to demonstrate its use as a readout system.

The results of the cryogenic measurement are shown in Fig. 5. The de-embedding of the existing coaxial readout chain is imperfect, because we cannot perform a calibration routine at the mixing chamber stage. Instead, we compared two measurements performed in separate cooldowns. One measurement is with the device installed, and a second measurement is with the device removed. In the latter case, the readout chain is shorted using the Tabbi/$^{\mathrm{TM}}$2Flex connectors that normally would connect to the device. By substracting the latter measurement from the former, the transmission through the flexline connectors and the chip

can be measured with the reference planes at the Tabbi/$^{\mathrm{TM}}$2Flex ends of the flexline connector. This substraction does not take into account small phase differences that might have occurred between the two measurements, and this results in imperfect de-embedding of the measurement.

The results show that our measured transmission across the flexline connector is somewhat worse than what is expected based on the simulation and the probe station measurement. This might be due to the poor de-embedding procedure, however, we must also note that the setup uses two SMA blocks and two Tabbi/$^{\mathrm{TM}}$2Flex connectors to connect to our system, which could cause the small amount of extra losses. The Tabbi/$^{\mathrm{TM}}$2Flex connectors simply press two ends of a flexline with exposed leads together within a metal block to make contact. During our cryogenic tests we have observed some connectors of the flexline readout lines making unreliable contacts, causing more contact losses than usual. Since the de-embedding is not ideal, we cannot distinguish if this is the true cause of the additional losses, versus the de-embedding procedure adding losses or the flexline connector having worse losses than expected. In any case, we are able to make contact across the two flexline connectors and demonstrate its use as a KID readout.

V. Conclusion

We have demonstrated a flexline-to-chip transition for larger scale cryogenic systems that allows the direct transition from flexline to device. The design has taken special care in reliability in the cryogenic environment and is made as light-tight as possible. Furthermore, the small footprint and easy interchangibility of chips make it a very flexible readout system. The design was verified using a probe station measurement and a cryogenic measurement. We get close to the expected transmission across our flexline connector, with a small additional loss due to contact losses. In short, the flexline connector has shown to be perfectly capable to act as reliable interface between flexline and chip, for example in a KID array. Advances such as these make compact chips with arrays of over 10 000 KIDs or with hundreds of qubits easier and less time consuming to test and operate, accelerating developments in these areas. By collaborating with Delft-Circuits on this development, the design presented here is easily refined for commercial success, providing our community with a new compact and integrated flexline readout system from end to end.

V. Acknowledgment

The authors would like to thank Juan Bueno for providing the probe station and assisting with the probe station measurements.

References

[1] R. Acharya et al., "Quantum error correction below the surface code threshold," *Nature*, vol. 638, no. 8052, pp. 920–926, Feb. 2025.

[2] M. Kjaergaard et al., "Superconducting qubits: Current state of play," *Annu. Rev. Condens. Matter Phys.*, vol. 11, pp. 369–395, 2020.

[3] J.-H. Yeh, J. LeFebvre, S. Premaratne, F. C. Wellstood, and B. S. Palmer, "Microwave attenuators for use with quantum devices below 100 mK," *J. Appl. Phys.*, vol. 121, no. 22, Jun. 2017, Art. no. 224501.

[4] S. Krinner et al., "Engineering cryogenic setups for 100-qubit scale superconducting circuit systems," *EPJ Quantum Technol.*, vol. 6, no. 1, Dec. 2019, Art. no. 2.

[5] J. C. Brennan et al., "Classical interfaces for controlling cryogenic quantum computing technologies," *APL Quantum*, vol. 2, no. 4, Dec. 2025, Art. no. 041501.

[6] Z. D. Kermish et al., "The POLARBEAR Experiment," in *Millimeter, Submillimeter, and Far-Infrared Detectors and Instrumentation for Astronomy VI*, vol. 8452. Bellingham, WA, USA: SPIE, 2012, pp. 366–380.

[7] W. B. Doriese et al., "Developments in time-division multiplexing of X-ray transition-edge sensors," *J. Low Temp. Phys.*, vol. 184, no. 1, pp. 389–395, Jul. 2016.

[8] L. Ferrari et al., "Antenna coupled MKID performance verification at 850 GHz for large format astrophysics arrays," *IEEE Trans. THz Sci. Technol.*, vol. 8, no. 1, pp. 127–139, Jan. 2018.

[9] J. Bueno, V. Murugesan, K. Karatsu, D. J. Thoen, and J. J. A. Baselmans, "Ultrasensitive kilo-pixel imaging array of photon noise-limited kinetic inductance detectors over an octave of bandwidth for THz astronomy," *J. Low Temp. Phys.*, vol. 193, no. 3/4, pp. 96–102, Nov. 2018.

[10] A. N. Bender et al., "Integrated Performance of a Frequency Domain Multiplexing Readout in the SPT-3 G Receiver," in *Millimeter, Submillimeter, and Far-Infrared Detectors and Instrumentation for Astronomy VIII*, vol. 9914. Bellingham, WA, USA: SPIE, 2016, pp. 321–331.

[11] M. Meschke, W. Guichard, and J. P. Pekola, "Single-mode heat conduction by photons," *Nature*, vol. 444, no. 7116, pp. 187–190, Nov. 2006.

[12] J. P. Smith et al., "Flexible coaxial ribbon cable for high-density superconducting microwave device arrays," *IEEE Trans. Appl. Supercond.*, vol. 31, no. 1, Jan. 2021, Art. no. 2500105.

[13] J. P. Smith, B. A. Mazin, A. Boaventura, K. J. Thompson, and M. Daal, "Improved flexible coaxial ribbon cable for high-density superconducting arrays," *IEEE Trans. Appl. Supercond.*, vol. 34, no. 2, pp. 1–6, Mar. 2024.

[14] G. A. Hernandez et al., "Microwave performance of Niobium/Kapton superconducting flexible cables," *IEEE Trans. Appl. Supercond.*, vol. 27, no. 4, Jun. 2017, Art. no. 1200104.

[15] A. B. Walter, C. Bockstiegel, B. A. Mazin, and M. Daal, "Laminated NbTi-on-Kapton microstrip cables for flexible sub-kelvin RF electronics," *IEEE Trans. Appl. Supercond.*, vol. 28, no. 1, Jan. 2018, Art. no. 2500105.

[16] Spira Manufacturing, "Spira-Shield," *Spira Manuf.*, Accessed: Jan. 14, 2025. [Online]. Available: https://www.spira-emi.com/product/spira-shield/